JJEES

JJEES (2024) 15 (3): 183-191
ISSN 1995-6681

Jordan Journal of Earth and Environmental Sciences

b-value Estimation and Extreme Magnitude Assessment in the Source Region of Past Earthquakes in Central Himalaya and Vicinity

Ram Krishna Tiwari*, Harihar Paudyal

Birendra Multiple Campus, Tribhuvan University, Bharatpur, Chitwan, Nepal

Received Dec. 21th, 2023; Accepted Jan. 9th , 2024

Abstract

The Gutenberg-Richter (GR) and Gumbel methodologies were applied to analyze seismic activity parameters (specifically, b-values) in the central Himalaya region, covering latitudes between 26° and 31° E and longitudes between 80° and 88° N during the time frame from 1964 to 2021. Additionally, Gumbel's techniques were utilized to gauge the frequency of occurrence for moderate-tolargemagnitude earthquakes. Within a circular area with a diameter of 250 kilometers, we determined the b-values for the primary source regions of the ten past major earthquakes. The estimated b-value based on GR relation varies from 0.82±0.06 to 1.02±0.10, whereas the b-value based on Gumbel's method ranges from 0.86±0.30 to 1.88±0.32. The results indicate that Gumbel's distribution approach is effective for regions where large earthquake data is available, and the b-values, estimated from the GR method, are found to be more appropriate for the tectonics of the source regions. The Lo-Mustang earthquake region and Bajhang earthquake regions are identified as probable regions for the occurrence of a large earthquake in less than 100 years, which also supports the existence of a western Nepal seismic gap between Uttarakhand, India, and central Nepal. The findings describe the seismic risk in the epicenters of previous earthquakes in terms of b-value, recurrence intervals, and earthquake probability for each magnitude.

Keywords: *GR relation, Gumbel distribution, b-value, Central seismic gap*

1. Introduction

The central Himalayan and adjoining region, delineated by latitude 26°–31°N and longitude 80°–88°E,has been considered as the study region. This region includes Nepal's entire territory and some parts of India and China. The region can be traditionally classified into distinct tectonic divisions when moving from south to north (Yin, 2006) (Figure 1). These divisions include the Sub-Himalaya, Lesser Himalaya, Higher Himalaya, and Tethyan Himalaya. They are demarcated by the presence of four significant east-west trending faults, namely the Main Frontal Thrust (MFT), the Main Boundary Thrust (MBT), the Main Central Thrust (MCT), and the South Tibetan Detachment System (STDS) (Thakur et al., 2019). Tanakpur Lineament (TL), Karnali Lineament (KL), and Samea Lineament (SL) are the transverse lineaments in western Nepal (Tiwari and Paudyal, 2023a). In contrast, Judi Lineament (JL), Thaple Lineament (TL), Kathmandu Lineament (KTML), Motihari-GauriShanker Lineament (MGL), Motihari-Everest Lineament (MEL), Arun Lineament (AL), and Kanchenjunga Lineament (KANL) are lineaments from central Nepal to eastern Nepal (Tiwari et al., 2022).

The central portion of the Himalayan Mountain range has witnessed a series of catastrophic earthquakes, as outlined in Table 1. One such event was the devastating 2015 Gorkha earthquake, which registered a magnitude of 7.8 on the Richter scale. This earthquake had profound impacts, resulting in approximately 9,000 fatalities and the destruction of over fifty thousand structures, leading to substantial economic losses in the affected region (Bilham, 2019; Wyss and Chamlagain, 2019). While the Gorkha Earthquake was significant, it was smaller in magnitude, compared to the great earthquakes that have been anticipated in central Nepal (Bilham et al., 2017; Hussain et al., 2020; Morell et al., 2017). Puzzlingly, this event raised the probability of more catastrophic earthquakes, occurring in the future along the Himalayan orogenic belt.

The main objective of the present study is to estimate the b-value, using the Gutenberg-Richter (GR) and Gumbel methods, establishing a connection between b-values and tectonics, and determining earthquake recurrence probabilities in the central Himalayas and its surroundings.

B-value by Gutenberg-Richter

The b-value of GR relation (Gutenberg and Richter, 1944) is the slope of the equation

$$\log N(M) = a - bM \quad (1)$$

Where the seismicity metric N(M) indicates the cumulative count of earthquakes that have a magnitude equal to or greater than the completeness threshold M, additionally, a metric "a" is used to quantify seismicity (Ahmed et al., 2021; Tiwari and Paudyal, 2022, 2021). Another important factor is known as the b-value, which quantifies the frequency of small and large earthquakes, occurring within a specific region (Ahmed et al., 2021; Amelung and King, 1997).

* Corresponding author e-mail: ram.tiwari@bimc.tu.edu.np

The b-value is influenced by various factors. For instance, an increase (or decrease) in stress applied to a geological volume will result in a corresponding decrease (or increase) in the b-value (Jordan et al., 2019; Schorlemmer et al., 2005; Wang et al., 2021; Wiemer and Wyss, 2002). The b-value is closely connected to various aspects of crustal deformation, including faulting, cracking, folding, and fracturing, as well as processes like liquid migration and magmatic intrusions (Chen et al., 2006; Numan and Ghaeb, 2019; Scholz, 1968; Tiwari and Paudyal, 2023a). It also exhibits associations with tectonic features and focal mechanisms, with distinct fault regimes corresponding to different b-values. Typically, in strike-slip faulting, the b-value is around 1.0, whereas in normal faulting, it tends to be greater than 1.0, and in thrust faulting regimes, it is usually less than 1.0 (Abed et al., 2023; Amelung and King, 1997; Gulia and Wiemer, 2010; Tiwari and Paudyal, 2022). Furthermore, the b-value is greater than one for earthquake swarms (Aswini et al., 2021; Tiwari and Paudyal, 2023b).

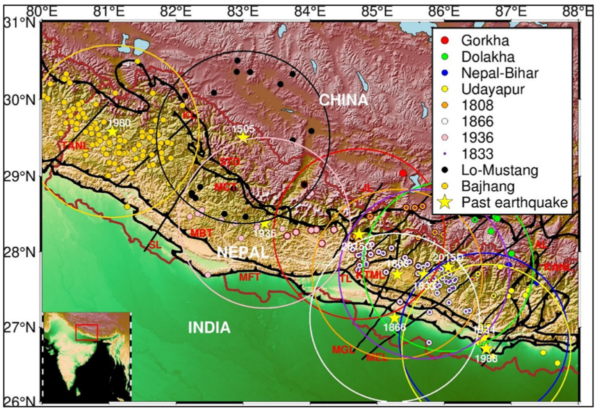

Figure 1. Tectonic map and source region of past earthquakes (yellow stars) inscribed by different colors circle. The center of the circle is at the epicenter location of earthquakes. MCT, MBT, and MFT are major thrust faults in the Himalayas, namely, Main Central Thrust, Main Boundary Thrust, and Main Frontal Thrust. TL, KL, and SL are Tanakpur Lineament, Karnali Lineament, and Samea Lineament, respectively. Other lineaments from central Nepal to eastern Nepal are Judi Lineament (JL), Thaple Lineament (TL), Kathmandu Lineament (KTML), Motihari-GauriShanker Lineament (MGL), Motihari-Everest Lineament (MEL), Arun Lineament (AL), and Kanchenjunga Lineament (KANL) (Öztürk et al., 2008; Shanker et al., 2007; Yadav et al., 2015).

B-value by the Gumbel method

Gumbel distribution is a probability distribution that models the maximum or minimum value of a set of random variables. In the context of earthquakes, it can be utilized to gauge the likelihood of the most significant seismic event that could occur within a specific region over a defined time. This probability estimation is directly derived from the premise that earthquakes originate from a straightforward Poisson process and adhere to the Gutenberg-Richter relation (Epstein and Lomnitz, 1966; Kijko and Ahjos, 1985). The earthquake distribution, based on the Gumbel distribution, is given as

$$G(M) = \exp\left(-\alpha e^{(-\beta M)}\right), M \geq 0 \tag{2}$$

The linear form of the equation is

$$\ln(-\ln G(M)) = \ln(\alpha) - \beta M \tag{3}$$

Where $G(M)$ represents the probability of earthquakes with magnitudes not exceeding M within a one-year timeframe, α represents the average annual count of earthquakes with a magnitude greater than 0, while β stands for the reciprocal of the average magnitude of earthquakes occurring in the specific region under consideration. Finally, M denotes the magnitude or intensity of an earthquake event. The coefficients of GR law and Gumbel distribution could be related as the following:

$$a = \frac{\ln \alpha}{\ln 10} \tag{4}$$

and

$$\mathrm{b} = \frac{\beta}{\ln 10} \tag{5}$$

Finally, the cumulative count of earthquakes (N) can be expressed as

$$N = \alpha e^{-\beta M} = -\ln[G(M)] \tag{6}$$

(Epstein and Lomnitz, 1966; Ray et al., 2019)

Mean or average return period

The mean return period stands as a crucial hazard parameter for any given geographic area (Ahmed et al., 2016; Al-Tarazi and Qadan, 1997; Husein et al., 1995). It quantifies the average time interval, denoted as T in years between occurrences of earthquakes with a magnitude surpassing M and given by

$$T = \frac{1}{N} = e^{\beta M}/\alpha \tag{7}$$

2. Material and Methods

The analysis in this study covers a period of 57 years (1964-2021), which ensures the reliability of quantitative analysis. The earthquake data was obtained from the International Seismological Center (ISC) catalog, containing 3153 earthquakes (Di Giacomo et al., 2018, 2015). To ensure accuracy, the catalog was declustered using the Reasenberg method (Reasenberg, 1985) in ZMAP software (Wiemer, 2001) with specific parameters: a confidence limit of 0.95, minimum magnitude cutoff of 1.5, interaction radius factor of 10, epicenter error of 1.5, and depth error of 2. This process resulted in the identification of 76 earthquake clusters, and after declustering, 2571 earthquakes were retained for analysis. To assess the completeness of the data, the maximum likelihood method was used, revealing a completeness magnitude of 4.5 mb. Therefore, the final dataset includes 478 earthquakes, all with a magnitude equal to or greater than the completeness value of 4.5 (Figure 2).

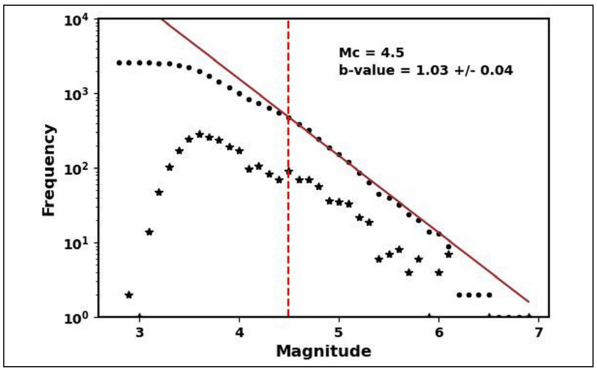

Figure 2. Magnitude of completeness (Mc) and b-value of frequency magnitude distribution where stars stand for non-cumulative frequency magnitude distribution. The b-value 1.03±0.04 shows that the study area is seismically active (Ghosh, 2020; Hamdache et al., 2018).

3. Results and Discussions

To compare the effectiveness of the approach to reflect the tectonic characteristics of the study area, b-values for the specified region were calculated from two methods namely, the Guttenberg and Richter frequency magnitude relationship approach (Gutenberg and Richter, 1944). Gumbel's annual extreme values method (Öztürk et al., 2008; Yadav et al., 2015) and details are presented in Table 1.

Table 1. The estimates of the GR parameter and Gumbel parameter in the source regions of the central Himalayan and adjoining region.

SN	Source region	Epicenter		No. of events	GR parameter			Gumbel parameter			
		Longitude	Latitude		a-value	b-value	R^2	β-value	R^2	b-value	R^2
1	Lo-Mustang earthquake (1505)	82.00°E	30.00°N	20	3.87	0.95 ±0.16	0.89	2.71 ± 0.00	0.72	1.18 ±0.00	0.72
2	1808 earthquake	86.63°E	26.71°N	66	4.03	0.87 ±0.09	0.68	2.26 ± 0.22	0.58	0.98 ±0.10	0.58
3	1833 earthquake	85.70°E	27.70°N	72	4.09	0.88 ±0.08	0.68	2.36 ± 0.19	0.58	1.02 ±0.08	0.58
4	1866 earthquake	85.26°E	27.12°N	55	4.61	1.02 ± 0.10	0.81	2.96 ± 0.28	0.62	1.28 ±0.12	0.62
5	Nepal-Bihar earthquake (1934)	86.59°E	26.86°N	44	3.75	0.85 ±0.10	0.78	2.17 ± 0.30	0.61	0.94 ±0.13	0.61
6	1936 earthquake	83.32°E	28.38°N	26	4.24	1.02 ±0.11	0.99	4.33 ± 0.74	0.82	1.88 ±0.32	0.82
7	Bajhang earthquake (1980)	81.05°E	29.58°N	103	3.96	0.82 ±0.06	0.89	2.79 ± 0.68	0.72	1.21 ±0.30	0.72
8	Udayapur earthquake (1988)	84.73°E	28.23°N	34	3.75	0.87 ±0.13	0.74	1.99 ± 0.69	0.57	0.86 ± 0.30	0.57
9	Gorkha earthquake (2015)	84.73°E	28.23°N	47	3.88	0.88±0.1	0.66	2.17 ± 0.67	0.56	0.94 ±0.29	0.56
10	Dolakha earthquake (2015)	86.06°E	27.80°N	70	4.23	0.91 ±0.08	0.87	2.94 ± 0.64	0.68	1.28 ±0.28	0.68

The b-values in 10 regions are exhibited in Figure 3, in which b-value is represented by the slope of the red solid line. The legend box in each image depicts b-values with the corresponding standard deviation, magnitude of completeness (Mc), and coefficient of determination (R^2). Evidently, Figure 3 shows the different b-values in each, suggesting different evolutions of stress states in different places. The 1866 and the 1936 earthquake regions were registered as areas with b-values 1.02±0.10, and 1.02±0.11, respectively, close to the global mean value of 1.0, whereas other regions were characterized as having a b-value less than 1.0, as shown in Figure 3. This increse suggests that the 1866 and 1936 earthquake regions were seismically active while other regions having comparative low b-values were more prone to seismic activity.

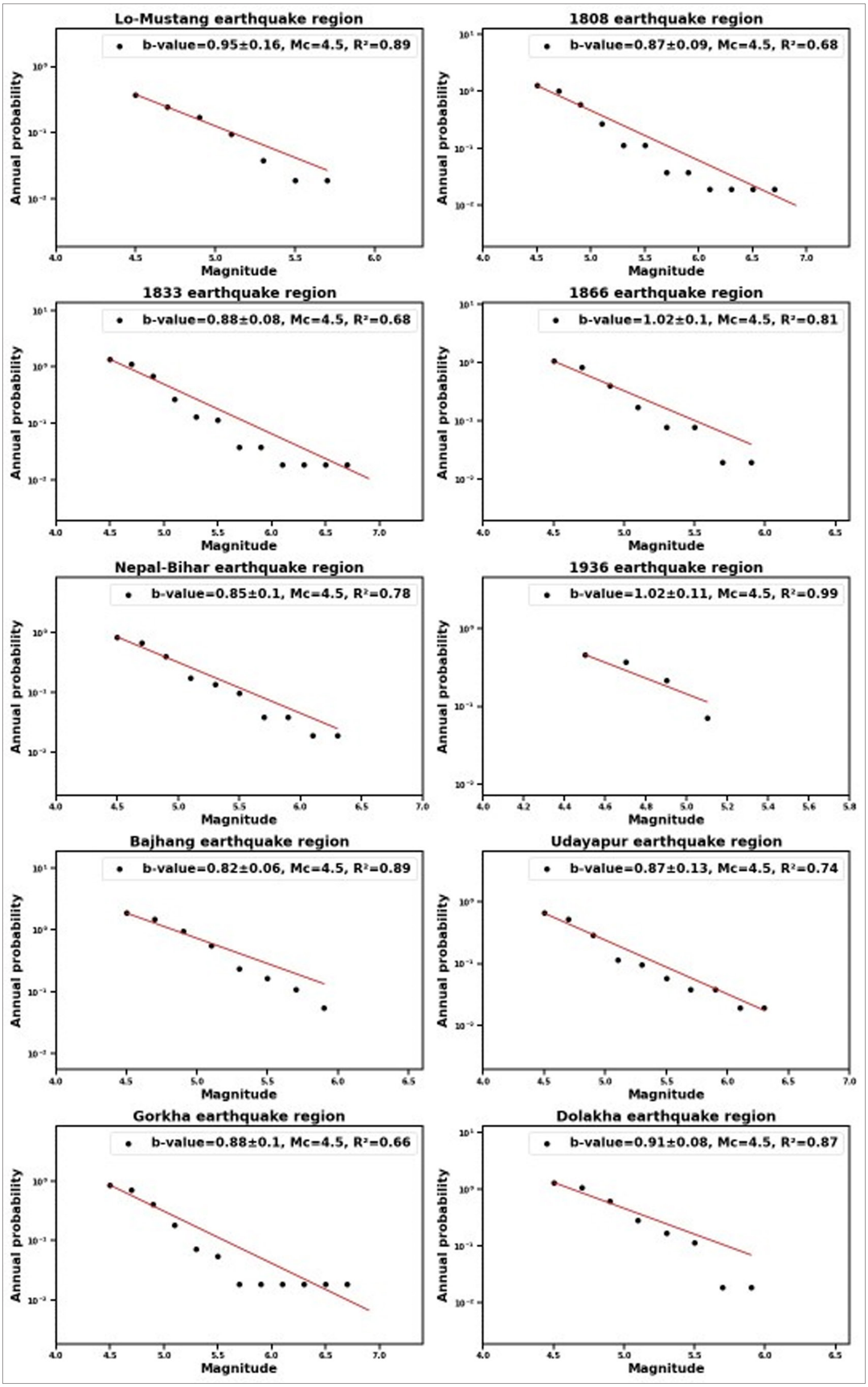

Figure 3. Frequency-Magnitude plot of the **(a)** Lo-Mustang earthquake region **(b)** 1808 earthquake region **(c)** 1833 earthquake region **(d)** 1866 earthquake region **(e)** Nepal-Bihar earthquake region **(f)** 1936 earthquake region **(g)** Bajhang earthquake region **(h)** Udayapur earthquake region **(i)** Gorkha earthquake region **(j)** Dolakha earthquake region

The highest β value (4.33 ± 0.74) or b value (1.88 ± 0.32) is observed in the 1936 earthquake region, while the lowest β value (1.99 ± 0.69) or b value (0.86 ± 0.30) is observed for Udayapur earthquake region (Figure 4). The subsequent high β values (2.96 ±0.28) or b value (1.28 ± 0.12) are observed in the 1866 earthquake and Dolakha earthquake regions (2.94 ± 0.64 or 1.28 ± 0.28). The earthquake regions of Nepal-Bihar and Gorkha show similar values of β =2.17 ± 0.30 or b value = 0.94 ± 0.13 and β= 2.17 ± 0.67 or b value = 0.94 ± 0.29, respectively, revealing a parallel style of tectonic stress accumulation, coupled with a low frequency of earthquake events. The source region of Lo-Mustang earthquake and Bajhang earthquake region show β value of 2.71 ± 0.00 or b value = 1.18 ± 0.00 and β value of 2.79 ± 0.68 or b value = 1.21± 0.30, respectively. The source region of the 1808 earthquake and the 1833 earthquake show β value of 2.26 ± 0.22 or b value = 0.98± 0.10 β and value of 2.36 ± 0.19 or b value of 1.02± 0.08, respectively. The variation in the estimated values, observed in our study, can likely be attributed to several factors, including disparities in earthquake data utilized for analysis, variations in the sizes of seismic zones, and differences in the applied analytical techniques.

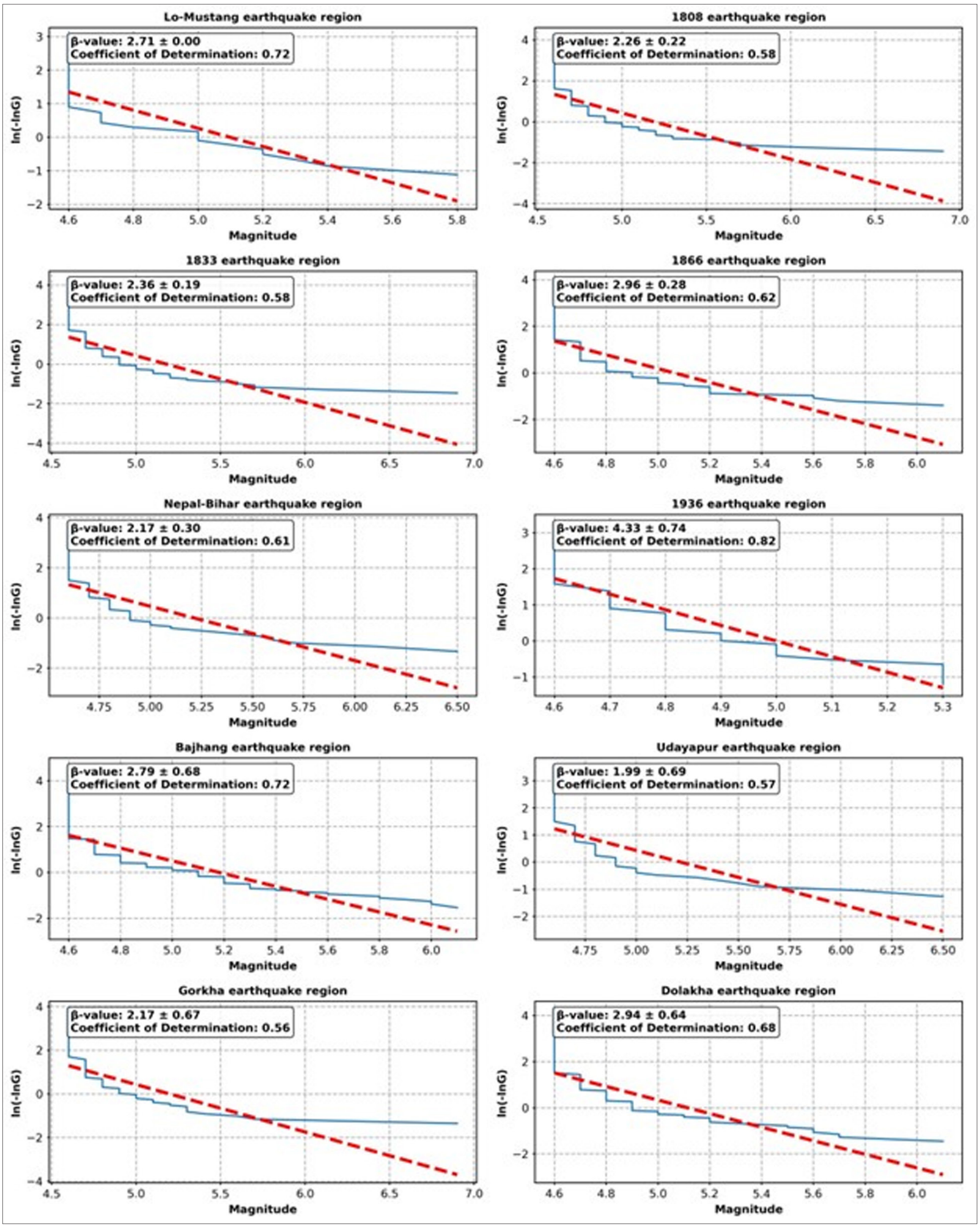

Figure 4. The Gumbel distribution characterization of the extreme values of the **(a)** Lo-Mustang earthquake region **(b)** 1808 earthquake region **(c)** 1833 earthquake region **(d)** 1866 earthquake region **(e)** Nepal-Bihar earthquake region **(f)** 1936 earthquake region **(g)** Bajhang earthquake region **(h)** Udayapur earthquake region **(i)** Gorkha earthquake region **(j)** Dolakha earthquake region.

The mean return period curves for 10 different regions are plotted in Figure 5. The 1808, 1833, 1866 the Nepal-Bihar, the Udayapur, the t and the Gorkha earthquake regions, exhibit a reduced likelihood of earthquake occurrences and extended return periods when compared to other zones, indicating a lower susceptibility to future moderate seismic events. The remaining regions are seismically active in terms of return periods. The mean return period for a magnitude 5.8 earthquake is estimated to be 85–90 years in the Lo-Mustang region. A return period of around 12 years for magnitude 5.2 is expected for the 1936 earthquake region. A return period of around 90 years is expected for the Bajhang earthquake region, while a return period of more than 250 years is expected for magnitude 6 earthquakes in the Dolakha earthquake region. Observing the study region, it is evident that there are pockets of very high seismicity and other small areas of comparatively less activity.

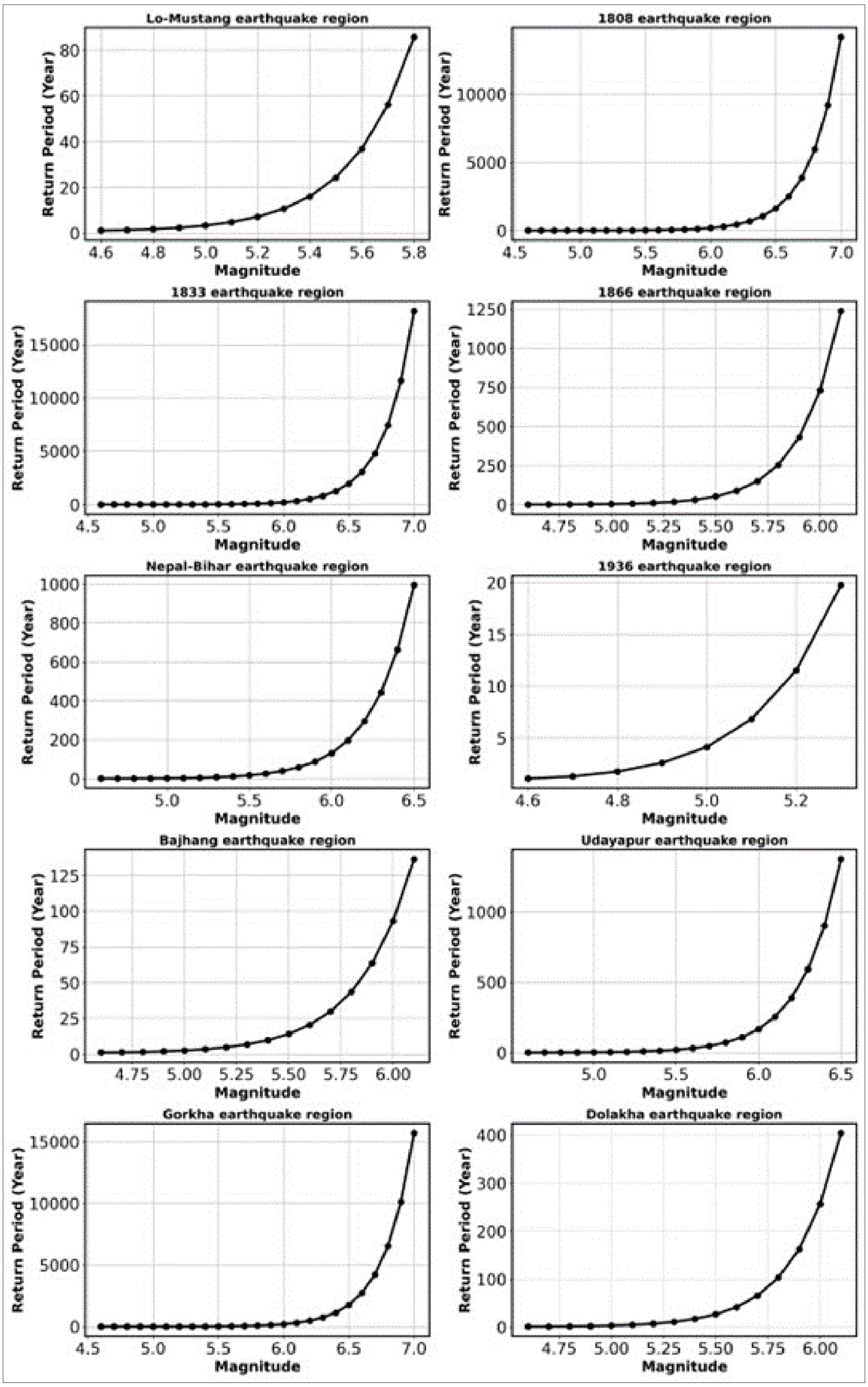

Figure 5. The average time intervals anticipated for specific magnitudes for **(a)** Lo-Mustang earthquake region **(b)** 1808 earthquake region **(c)** 1833 earthquake region **(d)** 1866 earthquake region **(e)** Nepal-Bihar earthquake region **(f)** 1936 earthquake region **(g)** Bajhang earthquake region **(h)** Udayapur earthquake region **(i)** Gorkha earthquake region **(j)** Dolakha earthquake region.

The exceedance curve [1-G(m)] represents the annual probability of an earthquake magnitude (Figure 6) surpassing a given value across various seismic source regions. Figure 6 shows that the cumulative probability distribution for exceedance, 1- G(m) of magnitudes ≤ 4.9 is greater than 50% and a distribution curve for non-exceedance is less than 50% for the regions considered.

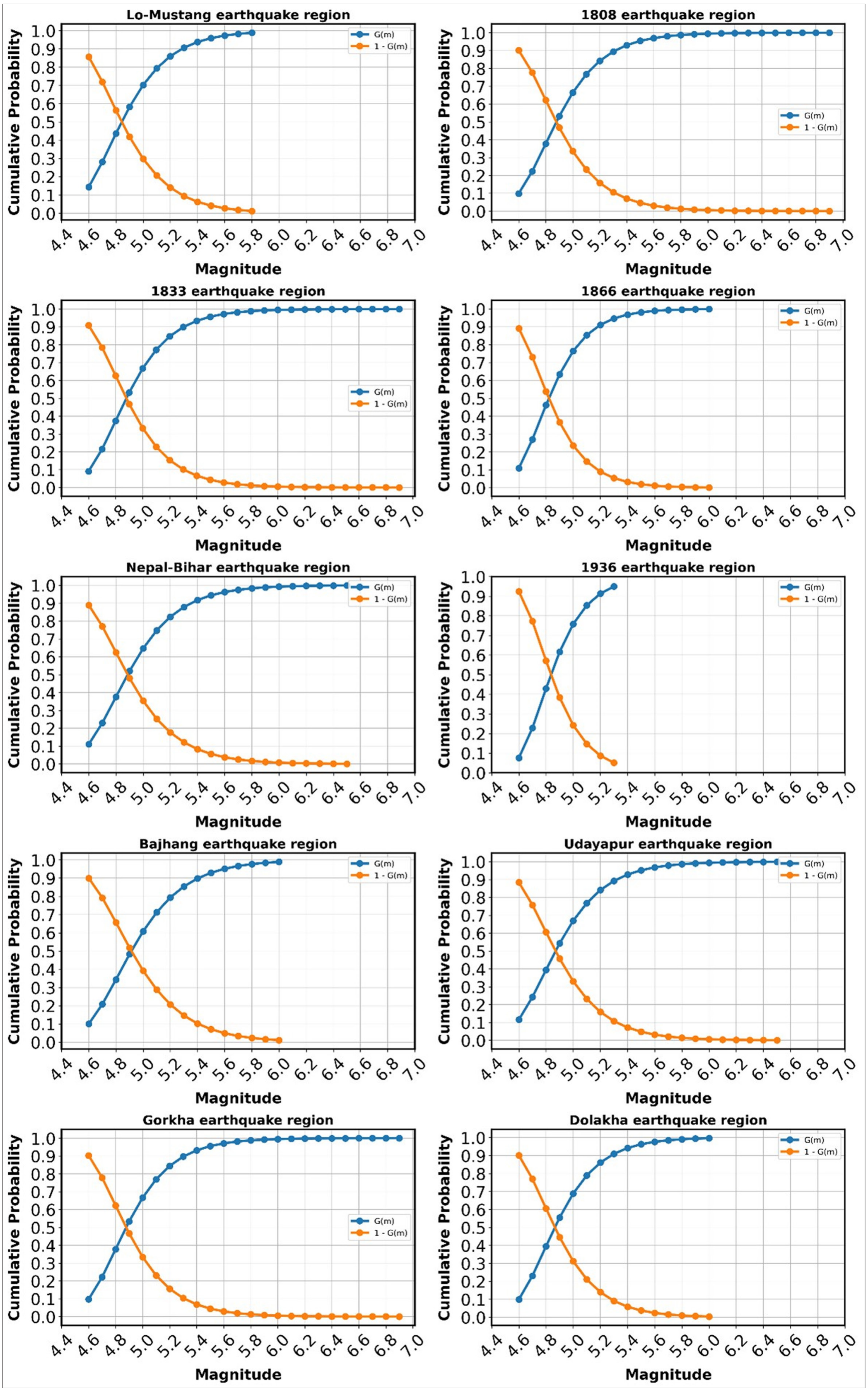

Figure 6. Probability of non-exceedance [G(m)] and exceedance [1-G(m)] for **(a)** Lo-Mustang earthquake region **(b)** 1808 earthquake region **(c)** 1833 earthquake region **(d)** 1866 earthquake region **(e)** Nepal-Bihar earthquake region **(f)** 1936 earthquake region **(g)** Bajhang earthquake region **(h)** Udayapur earthquake region **(i)** Gorkha earthquake region **(j)** Dolakha earthquake region.

In comparison to past research, the b-values were estimated in the ranges 0.88 to 1.08, 0.77 to 1.08, and 0.71 to 0.96 in the western, central, and eastern Nepal, respectively after 2015 Gorkha earthquake (Gunti et al., 2022). The study reveals that anticipated annual magnitude of the largest earthquakes in the Himalayan thrust zone are close to 5.5 (Yadav et al., 2011). Furthermore, it is estimated that the most probable annual earthquakes in the region 25º- 34ºN and 73º-85º E is 5.0 in magnitude with a probability of occurrence exceeding 50% annually (Shanker et al., 2007).

In conclusion, the b-values for the past 10 major earthquake source regions (central Himalaya and vicinity) are estimated through both GR relation and Gumbel's extreme value method. Furthermore, the return period of earthquake and assessment of extreme magnitude of the earthquake of same regions are estimated through Gumbel extreme value method. The estimated b-value through GR method varies from 0.82±0.06 to 1.02±0.10whereas b-value through Gumbel's method ranges from 0.86±0.30 to 1.88±0.32. The high b-value (1.88±0.32), estimated for the 1936 earthquake region (Gumbel's method), does not seem suitable, which may be because of inadequate earthquake events and lack of historical data. In general, it can be concluded that the b-values, estimated using the Gutenberg-Richter (GR) approach, provide a more accurate reflection of the tectonic characteristics in the studied area, whereas Gumbel's distribution approach found effective for the regions where large events are available. Based on the findings, it can be inferred that both the Lo-Mustang and the Bajhang earthquake regions are potential locations for experiencing a significant earthquake in less than 100 years. These regions in a western Nepal seismic gap between Uttarakhand and central Nepal and has not been visited by a large earthquake since 1505.

Conflict of Interests

The authors declare no conflict of interest

References

Abed, A.M., Al-Halboosi, J.M., Al-Jibouri, A.S., Al-Hetty, S. O. (2023). 2D Seismic Stratigraphic Analysis of Harthaand Kifl Formations in Balad Area– Center of Iraq. Jordan Journal of Earth and Environmental Sciences, 14(1):64–69.

Ahmed, J., Javed, F., Zafar, W.A., Iqbal, T., Shah, M.A. (2021). Spatial variation of b-value, creep rate, and seismic moment release along Chaman fault system. Arabian. Journal of Geosciences, 14:1623.

Ahmed, N., Ghazi, S., Khalid, P. (2016). On the variation of b-value for Karachi region, Pakistan through Gumbel's extreme distribution method. Acta Geodaetica et Geophysica, 51:227–235.

Al-Tarazi, E., and Qadan, H. (1997). Seismic hazard potential expected for the dams in Jordan. Natural and Engineering Sciences, 24(2).

Amelung, F., and King, G. (1997). Earthquake scaling laws for creeping and non-creeping faults. Geophysical Research Letters, 24: 507–510.

Aswini, K.K., Kamesh Raju, K.A., Dewangan, P., Yatheesh, V., Singha, P., Ramakrushana Reddy, T. (2021). Seismotectonic evaluation of off Nicobar earthquake swarms, Andaman Sea. Journal of Asian Earth Science, 221:104948.

Bilham, R. (2019). Himalayan earthquakes: A review of historical seismicity and early 21st century slip potential. Geological Society Special Publication. 483:423–482.

Bilham, R., Mencin, D., Bendick, R., Bürgmann, R. (2017). Implications for elastic energy storage in the Himalaya from the Gorkha 2015 earthquake and other incomplete ruptures of the Main Himalayan Thrust. Quaternary International, 462:3–21.

Chen, C.C., Wang, W.C., Chang, Y.F., Wu, Y.M., Lee, Y.H. (2006). A correlation between the b-value and the fractal dimension from the aftershock sequence of the 1999 Chi-Chi, Taiwan, earthquake. Geophysical Journal International, 167:1215–1219.

Di Giacomo, D., Bondár, I., Storchak, D.A., Engdahl, E.R., Bormann, P., Harris, J. (2015). ISC-GEM: Global Instrumental Earthquake Catalogue (1900-2009), III. Re-computed MS and mb, proxy MW, final magnitude composition and completeness assessment. Physics of the Earth and Planetary Interiors. 239:33–47.

Di Giacomo, D., Robert Engdahl, E., Storchak, D. A. (2018). The ISC-GEM Earthquake Catalogue (1904-2014): Status after the Extension Project. Earth System Science Data, 10(4):1877–1899.

Epstein, B., Lomnitz, C. (1966). A Model for the Occurrence of Large Earthquakes. Nature, 211:954–956.

Ghosh, U. (2020). Seismic Characteristics and Seismic Hazard Assessment: Source Region of the 2015 Nepal Earthquake Mw 7.8 in Central Himalaya. Pure and Applied Geophysics, 177:181–194.

Gulia, L., and Wiemer, S. (2010). The influence of tectonic regimes on the earthquake size distribution: A case study for Italy. Geophysical Research Letters, 37:1–6.

Gunti, S., Roy, P., Narendran, J., Pudi, R., Muralikrishnan, S., Vinod Kumar, K., Subrahmanyam, M., Israel, Y., Satish Kumar, B. (2022). Assessment of geodetic strain and stress variations in Nepal due to 25 April 2015 Gorkha earthquake: Insights from the GNSS data analysis and b-value. Geodesy and Geodynamics, 13:288–300.

Gutenberg, B., and Richter, C.F. (1944). Frequency of earthquakes in California. Bulletein of the Seismological Society of America. 34, 185–188.

Hamdache, M., Peláez, J.A., Gospodinov, D., Henares, J. (2018). Statistical Features of the 2010 Beni-Ilmane, Algeria, Aftershock Sequence. Pure and Applied Geophysics, 175:773–792.

Husein, A.I., Al-Homoud, A.S., Al-Tarazi, E., Nusier, O.K. (1995). Probabilistic seismogenic ground motion hazard assessment of Karak City in Jordan. Environmental & Engineering Geoscience. 1(2):207–218.

Hussain, H., Shuangxi, Z., Usman, M., Abid, M. (2020). Spatial variation of b-values and their relationship with the fault blocks in the western part of the tibetan plateau and its surrounding areas. Entropy, 22(9).

Jordan, N.W., Abutaha, S., Atallah, M., Abed, A. (2019). Structural Evolution of Wadi Hudaydun in Wadi Shueib Area, NW Jordan. Jordan Journal of Earth and Environmental Sciences, 10(3):152–160.

Kijko, A., and Ahjos, T. (1985). Seismic hazard in Finland: evaluation of Mmax. Geophysica, 21(1):39-50

Morell, K.D., Sandiford, M., Kohn, B., Codilean, A., Fülöp, R.H., Ahmad, T. (2017). Current strain accumulation in the hinterland of the northwest Himalaya constrained by landscape analyses, basin-wide denudation rates, and low temperature thermochronology. Tectonophysics, 721:70–89.

Numan, N., and Ghaeb, F. (2019). Geological and Hydrogeological Implications of Gravity Data in the Aqra

Plain Iraqi Kurdistan Region. Jordan Journal of Earth and Environmental Sciences, 10(3):145–151.

Öztürk, S., Bayrak, Y., Çinar, H., Koravos, G.C., Tsapanos, T.M. (2008). A quantitative appraisal of earthquake hazard parameters computed from Gumbel I method for different regions in and around Turkey. Natural Hazards, 47:471–495.

Ray, S., Alam, M.J.B., Haque, M., Das, S.K., Tanmoy, B.B., Hasan, M.N. (2019). A study on b-value and investigation of seismic hazard in Sylhet seismic region, Bangladesh using Gumbel's extreme value distribution method. SN Applied Science, 1(5).

Reasenberg, P. (1985). Second-order moment of central California seismicity, 1969-1982. Journal of Geophysical Research Solid Earth, 90:5479–5495.

Scholz, C.H. (1968). The frequency-magnitude relation of microfracturing in rock and its relation to earthquakes. Bulletein of the Seismological Society of America, 58:399–415.

Schorlemmer, D., Wiemer, S., Wyss, M. (2005). Variations in earthquake-size distribution across different stress regimes. Nature, 437;539–542.

Shanker, D., Yadav, R.B.S., Singh, H.N. (2007). On the seismic risk in the Hindukush-Pamir-Himalaya and their vicinity. Current Science, 92:1625–1630.

Thakur, V.C., Jayangondaperumal, R., Joevivek, V. (2019). Seismotectonics of central and nw himalaya: Plate boundary–wedge thrust earthquakes in thin-and thick-skinned tectonic framework. Geological Society Special Publication, 481:41–63.

Tiwari, R.K., Paudyal, H. (2023a). Spatial mapping of b-value and fractal dimension prior to November 8 , 2022 Doti Earthquake, Nepal. PLoS One, 18:1–13.

Tiwari, R.K., Paudyal, H. (2023b). Fractal Characteristics of the Seismic Swarm Succeeding the 2015 Gorkha Earthquake , Nepal. Indian Geotechnical Journal, 53:789–804.

Tiwari, R.K., Paudyal, H. (2022). Frequency magnitude distribution and spatial correlation dimension of earthquakes in north-east Himalaya and adjacent regions. Geologos, 28:115–128.

Tiwari, R.K., Paudyal, H. (2021). Statistics of the earthquakes in the central Himalaya and its vicinity in last 56 years , with an emphasis in the 25 April 2015 Gorkha , Nepal earthquake. Contributions to Geophysics and Geodesy, 51:321–343.

Tiwari, R.K., Paudyal, H., Shanker, D. (2022). On the spatio-temporal variation in b-value after 25 April 2015 Gorkha, Nepal earthquake. Geodesy and Geodynamics, 13:525–533.

Wang, R., Chang, Y., Miao, M., Zeng, Z., Chen, H., Shi, H., Li, D., Liu, L., Su, Y., Han, P. (2021). Assessing earthquake forecast performance based on b value in yunnan province, China. Entropy, 23(6).

Wiemer, S. (2001). A software package to analyze seismicity: ZMAP. Seismological Research Letters, 72:373–382.

Wiemer, S., and Wyss, M. (2002). Mapping spatial variability of the frequency-magnitude distribution of earthquakes. Advances in Geophysics, 45(C).

Wyss, M., and Chamlagain, D. (2019). Estimated casualties in possible future earthquakes south and west of the M7.8 Gorkha earthquake of 2015. Acta Geophysica, 67(2):423–429.

Yadav, R.B.S., Koravos, G.C., Tsapanos, T.M., Vougiouka, G.E. (2015). A Probabilistic Estimate of the Most Perceptible Earthquake Magnitudes in the NW Himalaya and Adjoining Regions. Pure and Applied Geophysics, 172:197–212.

Yadav, R.B.S., Tripathi, J.N., Shanker, D., Rastogi, B.K., Das, M.C., Kumar, V. (2011). Probabilities for the occurrences of medium to large earthquakes in northeast India and adjoining region. Natural Hazards, 56:145–167.

Yin, A. (2006). Cenozoic tectonic evolution of the Himalayan orogen as constrained by along-strike variation of structural geometry, exhumation history, and foreland sedimentation. Earth-Science Reviews, 76:1–131.